

Characterization of C₅ Hydrocarbons Relevant to Catalysis

Stewart F. Parker,^{*,†} David Siegel,[‡] Neil G. Hamilton,^{‡,§} Josef Kapitán,^{‡,||} Lutz Hecht,[‡] and David Lennon[‡]

[†]ISIS Facility, STFC Rutherford Appleton Laboratory, Chilton, Didcot, Oxon OX11 0QX, United Kingdom

[‡]Department of Chemistry, Joseph Black Building, University of Glasgow, Glasgow, G12 8QQ, United Kingdom

 Supporting Information

ABSTRACT: A recent *in situ* infrared study on the selective hydrogenation of C₅ dienes and monoenes over a Pd/Al₂O₃ catalyst only reported incomplete vibrational assignments for some of the reagents, intermediates, and products encountered in that study. This work uses a combination of infrared absorption spectroscopy, Raman, and inelastic neutron scattering to characterize the vibrational spectra of pentane, 1-pentene, *cis*- and *trans*-2-pentene, *cis*- and *trans*-1,3-pentadiene, 1,4-pentadiene, cyclopentane, and cyclopentene. Ab initio calculations of the potential energy surface, geometry, and vibrational transition energies were performed and simulations of the vibrational spectra compared to the experimental data. Complete vibrational assignments for the majority of the molecules are presented. The potential for using gas-phase infrared measurements for studying heterogeneously catalyzed gas-phase reactions is also briefly considered.



INTRODUCTION

Alkene chemistry on the industrial scale is closely associated with refinery capacities and covers a wide range of chemical processes.¹ C₂–C₄ olefins dominate, although higher alkenes (C₅ to ca. C₁₈) are also industrially significant, with unbranched alkenes attracting increased interest because of the latter's link to products with favorable properties such as biodegradability. Whether the double bond is terminal or internal is crucial, since the market for terminal alkenes is greater, with a world manufacturing capacity in 1994 amounting to 2.2 Mtonne.¹ Dienes are also industrially significant, with C₄ and C₅ 1,3-dienes predominating and 1,3-butadiene being the most important.

Hydrogenation of C₄ alkenes and dienes has been extensively investigated.² C₅ molecules have been much less studied. Most investigations have focused on experiments that aim to define the composition and structure of species present on the catalyst surface.³ A variation of the technique that is less commonly used is to record the infrared spectrum of the gases present over a supported metal catalyst to define the composition of the reacting medium at any one time. The usual approach for monitoring such reactions is by chromatographic techniques (e.g., gas–liquid chromatography) or mass spectrometry. However, the *in situ* infrared technique offers the advantage that, providing the reacting components can be unequivocally identified within a mixture of gases, the spectrum provides information on gases that are in direct exchange with the catalyst surface. Moreover, it provides information on equilibria that describe how a particular reagent or product is partitioned between the adsorbed and the gaseous phases at any one time. Since all the observed components are in the gas phase, where the observed spectral intensity is not complicated by adsorption-related effects such as dipole coupling, quantification of the associated infrared bands can be readily accomplished as the infrared intensities conform to the Beer–Lambert law. While *in situ* infrared analysis

of heterogeneously catalyzed gas-phase reactions has limitations, in particular, spectral overlap may compromise quantification of particular gases, thereby preventing determination of a mass balance, it does have the advantage of being able to distinguish stereoisomers, so that the possibility of isomerization reactions can also be evaluated for a given reaction sequence. This approach has been employed successfully^{4,5} to study the hydrogenation and isomerization of C₅ alkenes over a working Pd(1%)/Al₂O₃ catalyst.

Figure 1 shows the chemical structures of the species that may be present in the gas phase over a working catalyst. The variety results from the use of a technical mixture of *cis*- and *trans*-1,3-pentadiene which contains cyclopentene as an impurity. This mixture approximates to a C₅ raffinate from a refinery, so it has industrial relevance. For the analysis of the gas-phase spectra to be useful, it is crucial to be able to assign unambiguously the infrared spectra of the species that may be present. To our considerable surprise, we found that many of the species had only been poorly characterized if at all. The aim of this paper is to provide a complete assignment of the internal modes of the compounds shown in Figure 1. We therefore measured gas-phase infrared spectra, liquid-phase Raman spectra, and solid state inelastic neutron scattering (INS) spectra of these compounds. Together, the three spectroscopic techniques provide access to all vibrational modes. The assignments are obtained by comparison of the spectra simulated for the compound by density functional theory.

EXPERIMENTAL AND THEORETICAL METHODS

Infrared spectra (10 scans at 0.5 cm^{−1} resolution, 500–4000 cm^{−1}, acquisition time 42 s) were recorded using

Received: September 29, 2011

Revised: November 14, 2011

Published: November 16, 2011

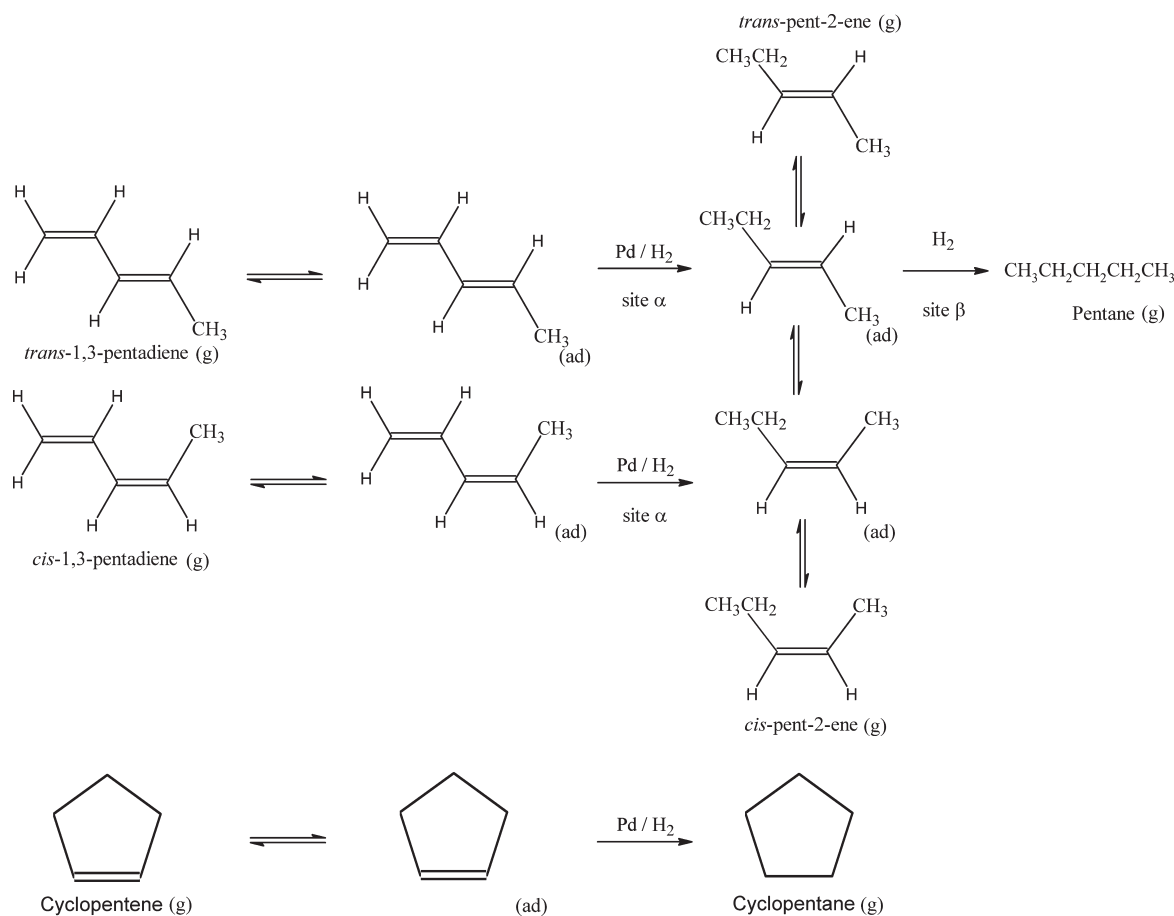


Figure 1. Scheme of the C5 species present over a working Pd/Al₂O₃ hydrogenation catalyst utilizing a mixed *cis*- and *trans*-1,3-pentadiene feedstock that contains cyclopentene as an impurity. Gas-phase species are denoted by (g) and adsorbed species by (ad). Adapted with permission from ref 5. Copyright 2010 Elsevier.

a Graseby-Specac 5661 continuous-flow heated gas cell (Specac Ltd., Orpington, U.K.) mounted on a custom-built socket in a Nicolet Avatar 360 infrared spectrometer. The beamline was constantly purged with dry, CO₂-free air.

The heated cell was flushed with helium and isolated (batch mode), and the compound was injected (as a liquid) through a septum using a glass/metal syringe. The temperature of the cell was maintained at 50 °C. Spectra were recorded for 10 μL injection volumes immediately after injection.

Liquid-phase Raman spectra (200–1900 cm⁻¹) were recorded on the custom-built GUROA3 spectrometer.⁶ This instrument is based on a fast stigmatic spectrograph HoloSpec HS-f/1.4 (Kaiser Optical Systems) equipped with a holographic transmission grating and back-thinned CCD detector (Wright Instruments, model P 312). The experimental parameters were as follows: room temperature (~293 K), 532 nm excitation wavelength, spectral resolution 6.5 cm⁻¹, and total acquisition time 25 s. Samples were held in specially manufactured 4 × 4 × 12 rectangular quartz (Spectrosil) microfluorescence cells (Optiglass) with an inner path length of 4 mm. The laser power at the sample was adjusted individually for each sample and was in the range 18–120 mW.

INS spectra⁷ were recorded using TOSCA⁸ at ISIS.⁹ TOSCA has high resolution, ~1.25% ΔE/E between 25 and 4000 cm⁻¹. In a cold room at -10 °C, the volatile C₅ compounds were loaded into aluminum cells sealed with indium gaskets. The cells

were subsequently carried in liquid nitrogen to the spectrometer and cooled to ~20 K, and spectra were recorded for 3–6 h. The INS spectra are available from the INS database at <http://wwwisis2.isis.rl.ac.uk/INSdatabase/>.

Pentane (≥99%), *cis*-2-pentene (98%), *trans*-1,3-pentadiene (96%), technical mixture of 1,3-pentadienes (90% purity, 35% *cis*, 65% *trans*), 1,4-pentadiene (99%), cyclopentane (99%), and cyclopentene (96%) were obtained from Aldrich. 1-Pentene (≥95%) and *trans*-2-pentene (99%) were obtained from Fluka. All samples were used as received.

Ab initio calculations of the geometry and vibrational transition energies were carried out using Gaussian 03¹⁰ with the B3LYP functional and AUG-cc-pVDZ basis set. Relaxed potential energy scans to locate conformers were carried out with the same functional and basis set. In a few cases, in order to obtain more accurate energy differences between conformers MP2/AUG-cc-pVDZ calculations were carried out. Relative energies (the lowest energy conformer is used as the zero of energy) of conformers quoted in the text are corrected for zero-point energy (ZPE); figures showing relative energy as a function of angle are not corrected for ZPE. Mode visualization of the results was realized with GaussView 3.09. The calculated INS spectra were generated from the Gaussian 03 output using the in-house program ACLIMAX¹¹ (available from <http://wwwisis2.isis.rl.ac.uk/instruments/tosca/software/tosca-software4727.html>).

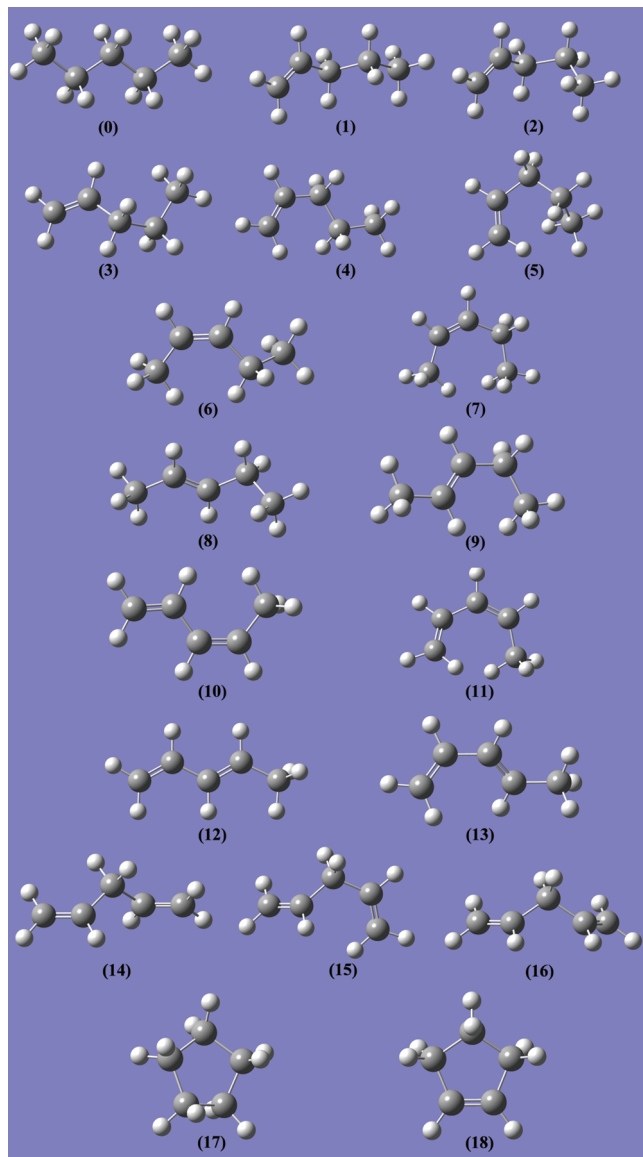


Figure 2. Chemical structures and conformations of the C₅ species considered in this work (the point group is given in square brackets). (0) *trans-trans*-pentane [C_{2h}], (1) 1-pentene conformer 1 (anti) [C₁], (2) 1-pentene conformer 2 (syn) [C₁], (3) 1-pentene conformer 3 [C₁], (4) 1-pentene conformer 4 [C₁], (5) 1-pentene conformer 5 [C₁], (6) *cis*-2-pentene skew conformer [C₁], (7) *cis*-2-pentene cis conformer [C₁], (8) *trans*-2-pentene skew conformer [C₁], (9) *trans*-2-pentene cis conformer [C_s], (10) *cis*-1,3-pentadiene s-trans conformer [C_s], (11) *cis*-1,3-pentadiene skew conformer [C₁], (12) *trans*-1,3-pentadiene s-trans conformer [C_s], (13) *trans*-1,3-pentadiene skew conformer [C₁], (14) 1,4-pentadiene C₂ conformer [C₂], (15) 1,4-pentadiene C₁ conformer [C₁], (16) 1,4-pentadiene C_s conformer [C_s], (17) cyclopentane [C_s] or [C₂, see text], and (18) cyclopentene [C_s] (19).

RESULTS AND DISCUSSION

For each of the molecules considered a comparison of the calculated structure with the available experimental data is given in the Supporting Information. We will present a comparison of observed and calculated spectra and a table of assignments for all molecules. Emphasis will be on those for which literature data is scarce or absent; for the better characterized systems the results are given in the Supporting Information. Figure 2 shows

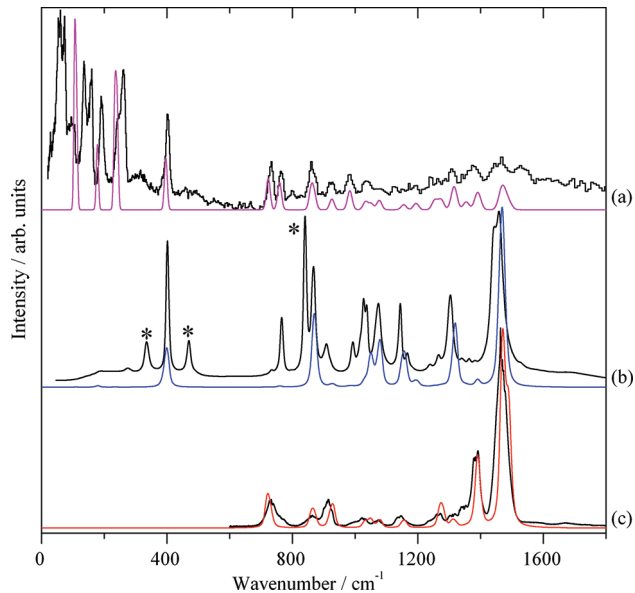


Figure 3. Comparison of measured (black traces) and calculated (in color) vibrational spectra of the *trans-trans* conformer of *n*-pentane (0): (a) INS, (b) Raman, and (c) infrared. Bands originating from the *trans-gauche* conformer are indicated by asterisks (*).

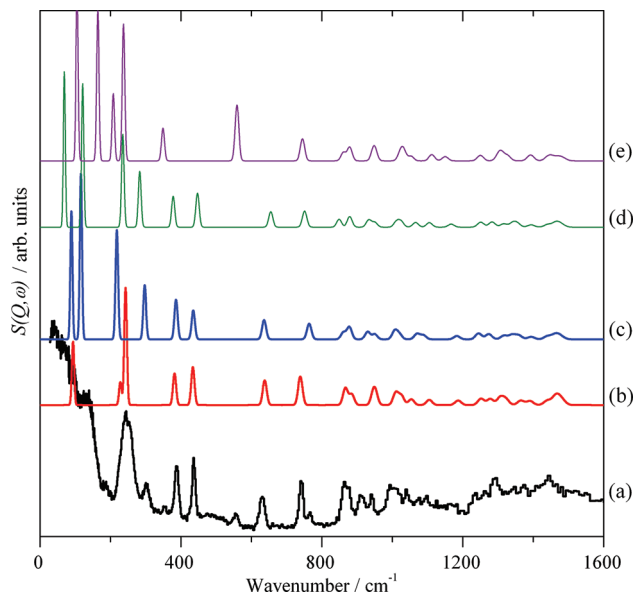


Figure 4. Comparison of (a) measured and calculated INS spectra of 1-pentene, (b) conformer 1 (1), (c) conformer 2 (2), (d) conformer 3 (3), and (e) conformer 4 (4).

the structures and conformations of all species considered in this work.

Pentane. Vibrational spectra of the *n*-alkanes,^{12–15} including pentane,¹⁶ have been extensively studied as model compounds for polyethylene.^{17,18} In the solid state pentane¹⁹ adopts the lowest energy *trans-trans* zigzag conformation, and the excellent match of the calculated INS spectrum of this conformer with that of the observed spectrum, Figure 3a, is consistent with this observation. Raman and infrared spectra are complicated by the presence of conformers^{12,13,20,21} that are energetically accessible at ambient and higher temperature. The presence of the

Table 1. Relative (the Lowest Energy Conformer Is Used as the Zero of Energy) Energies (kJ mol^{-1}) of Conformers of C5 Hydrocarbons

	B3LYP/AUG-cc-pVDZ, this work	MP2/AUG-cc-pVDZ, this work	MM3, ref 23	MP2/6-31G*, ref 23	MP2/6-311G*, ref 23	MP4/6-31G*, ref 23	MP4/6-311G*, ref 23
1-pentene							
conformer 1 (1)	0.00	0.59	0.00	0.41	0.72	0.00	0.00
conformer 2 (2)	3.13	0.00	0.49	0.00	0.00	0.28	0.08
conformer 3 (3)	5.05	3.16	1.77	3.30	3.07	3.28	2.89
conformer 4 (4)	6.30	2.81	3.19	3.82	4.03	2.78	2.81
conformer 5 (5)			6.33	7.58	7.66	7.00	7.00
<i>cis</i> -2-pentene							
skew conformer (6)	0.00						
<i>cis</i> conformer (7)	16.30						
<i>trans</i> -2-pentene							
skew conformer (8)	0.00						
<i>cis</i> conformer (9)	2.48						
<i>cis</i> -1,3-pentadiene							
s-trans conformer (10)	0.00						
skew conformer (11)	16.37						
<i>trans</i> -1,3-pentadiene							
s-trans conformer (12)	0.00						
skew conformer (13)	15.14						
1,4-pentadiene							
C_2 conformer (14)	0.00	0.00					
C_1 conformer (15)	3.18		4.06				
C_s conformer (16)	1.43		1.72				

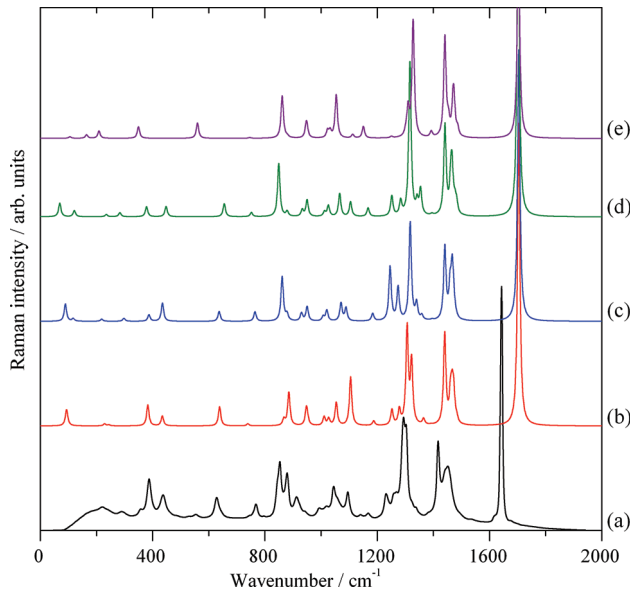


Figure 5. Comparison of (a) measured and calculated Raman spectra of 1-pentene, (b) conformer 1 (1), (c) conformer 2 (2), (d) conformer 3 (3), and (e) conformer 4 (4).

trans-gauche conformer is clearly seen in the Raman spectrum by the bands at 333, 468, and 839 cm^{-1} (marked with asterisks in Figure 3b). The infrared spectrum appears to be much less

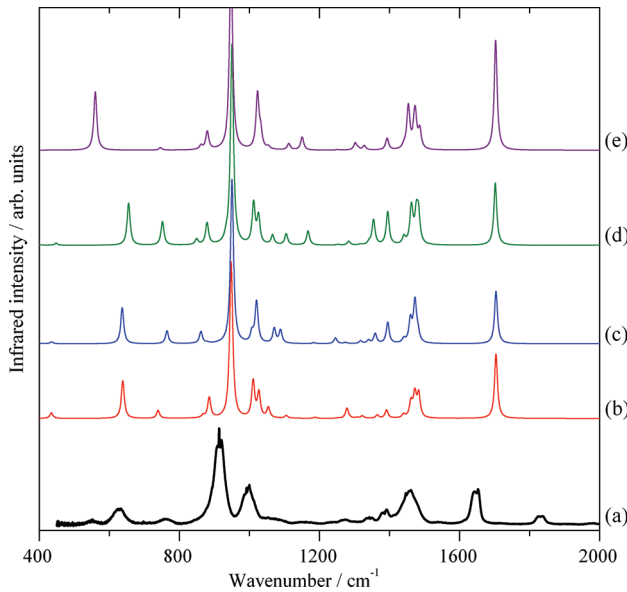


Figure 6. Comparison of (a) measured and calculated infrared spectra of 1-pentene, (b) conformer 1 (1), (c) conformer 2 (2), (d) conformer 3 (3), and (e) conformer 4 (4).

modified by the presence of conformers, probably because the conformer modes are masked by the broad rotational envelope of the modes of the trans-trans conformer. Table S1, Supporting

Information, lists the observed and calculated transition energies together with our assignments, which are in complete agreement with those of Mirkin and Krimm.¹⁶

Figure 3 confirms the results of a previous study²² regarding the intensities calculated by Gaussian 03, namely, that INS intensities are quantitative in the region above the lattice modes, infrared intensities are reliable, and Raman intensities should be regarded as being only semiquantitative, giving an indication of whether a mode is strong, medium, weak, or absent.

1-Pentene. For 1-pentene, the possibility of conformational isomerism also exists which has been investigated by microwave spectroscopy in the gas phase²³ and also theoretically.^{23,24} Investigation of the potential energy surface as a function of rotation about the C2–C3 and C3–C4 bonds finds five possible conformers.²³ These are shown in Figure 2 and are labeled according to a previous study.²³ Conformers 1 and 2 are in the anti and syn configurations, respectively.²⁴ The calculations find that conformers 1 and 2 are almost isoenergetic; the difference depends on the level of theory used. The highest levels of theory find the anti conformer to be the lowest in energy, but the difference between the two is generally less than $\sim 1 \text{ kJ mol}^{-1}$ ($\sim 100 \text{ cm}^{-1}$, $\sim 1/2kT$ at 300 K). The calculations²³ predict a ratio of 0.75:1.00:0.29:0.10:0.04 (for conformers 1–5) at room temperature, and the microwave data²³ is in qualitative agreement with the prediction. Conformer 5 was not observed, and the calculations show that it is much higher in energy than the other four conformers. There is also a very low energy path ($\ll kT$ at 300 K) from conformer 5 to conformer 3; both of these will disfavor conformer 5, and it will not be considered further.

We also examined this system using both DFT and MP2 calculations, and the results are shown in Table 1 together with those from the earlier study.²³ It is clear that there is a strong dependence on the choice of method.

Structural data for conformers 1–4 are listed in Table S2, Supporting Information. All bond distances and angles are as expected. The bond angles involving the sp^3 carbon atoms are almost tetrahedral. Calculated dihedral angles and rotational constants are in good agreement with those determined experimentally.²³

Investigation by infrared spectroscopy of 1-pentene in the liquid²⁵ and solid states²⁶ shows the presence of two conformers. As with pentane, it would be expected that the lowest energy conformer would be the only one found in the solid state. Unfortunately, the crystal structure of 1-pentene is not known. In addition, the persistence of conformers in the solid indicates that, as suggested previously,²⁶ it freezes to a glass rather than a crystal. The measured INS spectrum, Figure 4a, is consistent with this idea because, rather than the well-defined lattice modes found for pentane, there is an ill-defined lump indicating an absence of long-range order.

Figure 4 compares the experimental INS spectrum with those calculated for conformers 1–4. Only in the region $<200 \text{ cm}^{-1}$ do clear differences between the conformers exist. Since this is the region that the isolated molecule approximation inherent in Gaussian is least valid (since the internal and external modes mix) this makes distinguishing among them very difficult. The methyl torsion at 245 cm^{-1} is much broader (36 cm^{-1}) than the instrumental resolution ($\sim 4 \text{ cm}^{-1}$ at this energy), indicative of either dispersion in the mode (which is unlikely because there is no long-range order) or different environments consistent with multiple conformers. Conformer 2 is clearly present as shown by the band at 302 cm^{-1} (298 cm^{-1} calculated), as is conformer 4 as

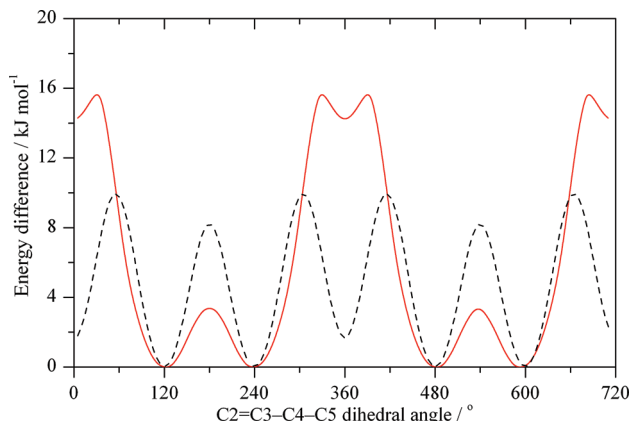


Figure 7. Potential energy surfaces for *cis*- (solid line) and *trans*-2-pentene (dashed line) as a function of rotation about the C3–C4 bond. The skew conformer (6,8) is found in the minima at 120° , 240° , 480° , and 600° , and the *cis* conformer is found in the minima at 0° , 360° , and 720° (7 and 9).

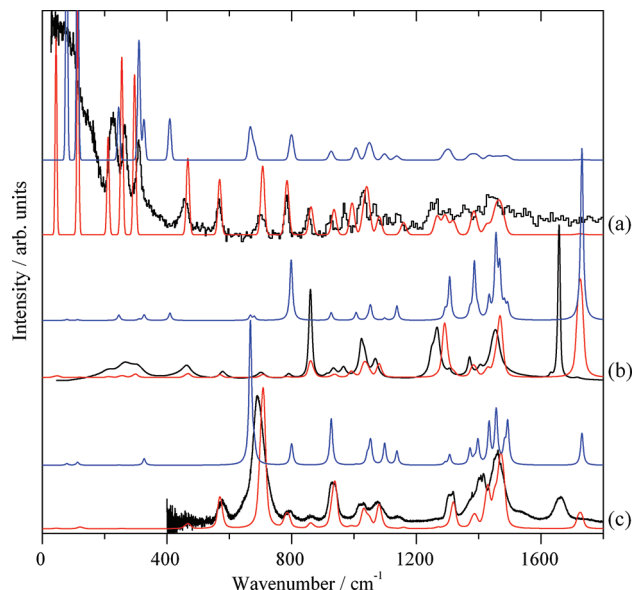


Figure 8. Comparison of measured (black traces) and calculated vibrational spectra for the skew (6, red) and *cis* (7, blue) conformers of *cis*-2-pentene: (a) INS, (b) Raman, and (c) infrared.

shown by the bands at 348 and 556 cm^{-1} (348 and 560 cm^{-1} calculated). These modes are all relatively weak, indicating that they are probably present only in small amounts. The intensity ratio of the two modes at 381 and 438 cm^{-1} is consistent with that predicted for conformer 1, suggesting that this is the major species, as found by the high-level ab initio calculations.²⁴

The liquid-phase Raman spectra shown in Figure 5 are also indicative of the presence of multiple conformers. This is most clearly seen by the doublet observed at $851/880 \text{ cm}^{-1}$; since none of the conformers have two strong bands at this position, at least two conformers are required to explain the data. Close inspection shows that the weak band measured at 557 cm^{-1} is characteristic of conformer 4, and that at 769 cm^{-1} is diagnostic of conformers 2 and 3. In the gas-phase infrared spectrum in Figure 6 the weak mode at 625 cm^{-1} , which is also seen in the

Table 2. Measured and Calculated Vibrational Transition Energies with Assignments for Conformers 1 (anti), 2 (syn), 3, and 4 of 1-Pentene^a

experimental/cm ⁻¹			DFT/cm ⁻¹				assignment
infrared	Raman	INS	conformer 1 (anti)	conformer 2 (syn)	conformer 3	conformer 4	
			93	89	69	165	C2–C3 torsion
			96	117	121	105	C3–C4 torsion
					209	C2–C3–C4 bend	
220w	246vs,br		229	218	235	237	methyl torsion + skeletal def.
290w	300w		244	298	283		C4 out-of-plane def. (TAM)
	352vw					350	C3–C4–C5 bend (LAM)
387m	389s		383	387	378		C3–C4–C5 bend (LAM)
438m	435s		435	435	447		C1–C2–C3 bend
546	556w					559	C1–C2–C3 bend
629	628m	630m	639	637	655	560	in-phase =CH out-of-plane bend
765	769w	740s	739			746	methylene rock (C3,C4) + methyl rock
765	769w	765w		765	752		methylene rock (C3,C4) + methyl rock
	853s	867s	867	879	879	880	methyl rock + methylene twist
	879s	874m	885	861	849	861	in-phase C–C stretches (C3–C4, C4–C5)
914	912m		947	950	950	947	vinyl CH ₂ wag
921	941w	935m	953	930	933	950	out-of-phase C–C stretches (C2–C3, C4–C5)
992	994vw		1011	1020	1012	1023	vinyl CH ₂ twist
1000	1019vw	1005s,br	1027	1011	1026	1032	vinyl CH ₂ rock
	1045m		1054	1071	1066	1054	out-of-phase C–C stretches (C3–C4, C4–C5)
						1112	out-of-phase methylene twists + methyl rock
	1095m		1105	1089	1105	1151	C–C stretch (C3–C4) + methyl rock
	1168vw		1187	1184	1167		C–C stretch (C2–C3) + vinyl CH ₂ rock
	1232m		1252	1246	1252	1250	out-of-phase methylene twists
1272	1264m		1279	1274	1283	1302	in-phase methylene wags
	1292vs	1293m	1307	1340	1341	1310	in-phase methylenic twists
	1304vs		1322	1317	1317	1327	vinyl CH in-plane bend
1343	1340vw		1365	1359	1354	1392	in-phase methylene wags
1388	1384vw		1392	1395	1395	1393	sym methyl HCH bend
	1418vs		1440	1441	1441	1441	out-of-phase vinyl CH ₂ scissors + methylene scissors (C3)
	1448vs		1461	1460	1462	1454	in-phase vinyl CH ₂ scissors + methylene scissors (C3)
			1467	1467	1467	1470	in-phase asym methyl HCH bend + methylene scissors (C4)
1460			1472	1473	1477	1473	asym methyl HCH bend
			1483	1481	1483	1487	out-of-phase asym methyl HCH bend + methylene scissors (C4)
1648	1643vs		1704	1704	1702	1703	=C=C stretch
1832							2 × 914 cm ⁻¹
2879			3000	3008	3002	2995	sym methylene stretch (C3)
2886			3024	3028	3027	3024	sym methyl stretch
2893			3025	3022	3026	3028	sym methylene stretch (C4)
			3046	3052	3060	3014	out-of-phase asym methylene stretch (C3,C4)
			3065	3061	3064	3062	asym methylene stretch (C4)
2940			3093	3094	3095	3092	asym methyl stretch
			3099	3106	3102	3098	asym methyl stretch
2967			3126	3123	3131	3129	vinyl CH stretch (C2)
2977			3135	3135	3143	3150	in-phase vinyl CH stretches (C1,C2)
3087			3224	3223	3223	3232	asym vinyl CH ₂ stretch

^as, strong; m, medium; w, weak; sh, shoulder; br, broad; v, very; sym, symmetric; asym, antisymmetric; LAM, longitudinal acoustic mode; TAM, transverse acoustic mode.

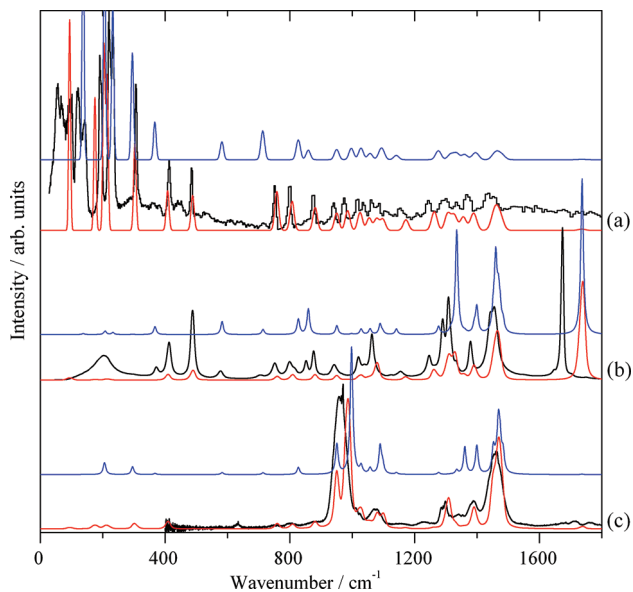


Figure 9. Comparison of measured (black traces) and calculated vibrational spectra for the skew (**8**, red) and cis (**9**, blue) conformers of *trans*-2-pentene: (a) INS, (b) Raman, and (c) infrared.

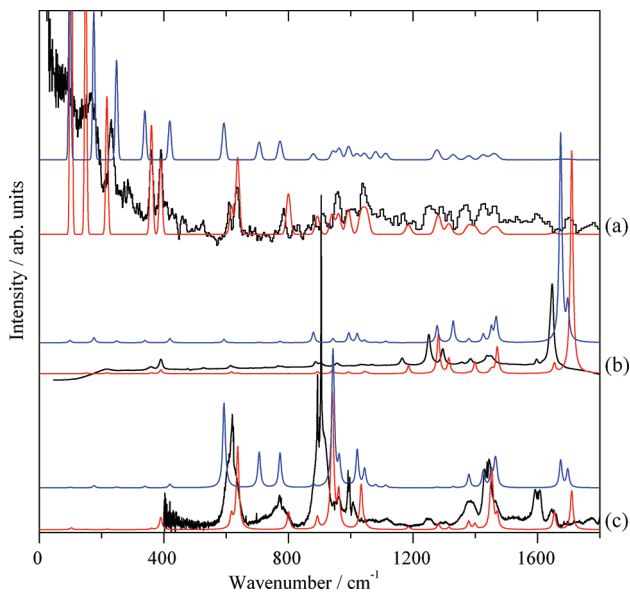


Figure 11. Comparison of measured (black traces) and calculated vibrational spectra for the skew (**10**, red) and cis (**11**, blue) conformers of *cis*-1,3-pentadiene: (a) INS, (b) Raman, and (c) infrared.

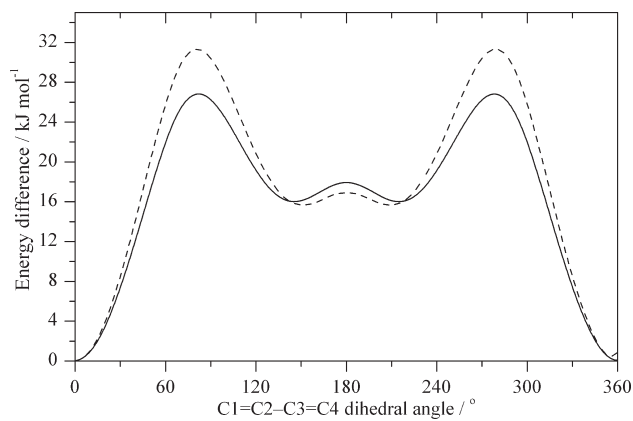


Figure 10. Potential energy surfaces for *cis*- (solid line) and *trans*-1,3-pentadiene (dashed line) as a function of rotation about the C2–C3 bond. The *s-trans* conformer (**10,12**) is found in the minima at 0° and 360°, the skew conformer is found in the minima at ~140° and ~220° (**11** and **13**), and the *s-cis* conformer is found at the saddle point at 180°.

liquid phase,²⁵ assigned to conformer 1 or 2 is present. In Table 2 we give the observed transition energies together with those calculated for conformers 1 (anti), 2 (syn), 3 and 4. As expected from the spectra the energies and assignments are very similar for conformers 1–3 and the modes are highly mixed. The C_s symmetry of conformer 4 imposes a clear distinction between some of the modes, e.g., methylene wags and twists, resulting in ‘purer’ modes.

In principle, it should be possible to test the reliability of the calculated relative energies by generating synthetic spectra with a ratio of conformers predicted by the calculations and assuming Boltzmann statistics. This was attempted for each of the vibrational spectroscopies but with little success. There are several factors that contribute to this ambiguous result. As seen in Table 1, the relative energies of the conformers are strongly dependent on the calculational method used (since the results

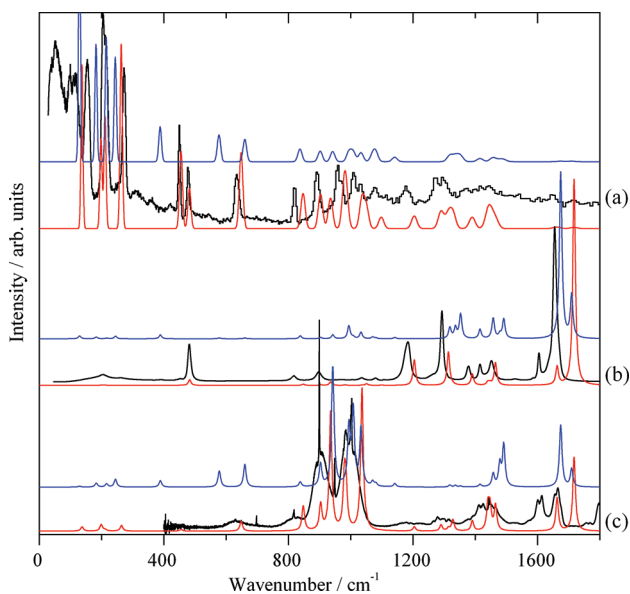


Figure 12. Comparison of measured (black traces) and calculated vibrational spectra for the skew (**12**, red) and cis (**13**, blue) conformers of *trans*-1,3-pentadiene: (a) INS, (b) Raman, and (c) infrared.

are the differences between very large numbers); thus, there is considerable uncertainty as to what is the ideal ratio of conformers. The major reason is that the spectra of the conformers are sufficiently similar to each other that varying the ratio of the components does not change the overall profile very much. The only conclusion that was obtained is that conformer 4 is present in the INS spectrum to a much higher extent than predicted by any of the calculations. This is probably because the distribution of conformers in the INS spectrum is probably not statistical because the sample is rapidly quenched in liquid nitrogen.

Comparison of the measured and calculated infrared and Raman spectra, Figures 5 and 6, shows that the calculations

Table 3. Measured and Calculated Vibrational Transition Energies with Assignments for *cis*-2-Pentene^a

experimental/cm ⁻¹			DFT/cm ⁻¹			assignment
infrared (gas phase, 323 K)	Raman (liquid, ~300 K)	INS (solid, 20 K)	skew conformer	cis conformer		
			46	79	C3—C4 torsion	
			123	113	C1 methyl torsion	
		227s	213	310	C5 methyl torsion	
	265w	261s	254	680	C3—C4—C5 bend	
	303w	311s	297	246	C2—C3—C4 bend	
468w	463w	454m	466	410	skeletal def. (pseudo-TAM)	
572m	578w	568m	570	327	C1—C2—C3 bend	
688s	700w	699m	707	668	in-phase cis =CH out-of-plane bend	
791w	791vw	785s	785	800	methylene rock + methyl rock (C5)	
861w	860vs	852	863	798	in-phase C—C stretch (C3—C4, C4—C5)	
934m	936w	921w	936	927	methyl rock (C1) + out-of-phase C—C stretch (C1—C2, C4—C5)	
		967w	963m	993	out-of-phase cis =CH out-of-plane bend	
1025m,br	1024m	1031	1032	1007	out-of-phase C—C stretch (C3—C4, C4—C5)	
			1040	1054	methyl rock (C1) + in-phase C—C stretches (C1—C2, C3—C4)	
			1047	1043	methyl rock (C1)	
1074m,br	1079w	1064w	1082	1098	methyl rock (C5)	
		1135w	1159	1138	methyl rock (C1)	
			1267	1293	methylene twist	
		1269s	1264m,br	1293	out-of-phase cis =CH in-plane bend	
1310m	1303vw		1318	1372	methylene wag	
1381	1372w	1357w	1384	1386	sym methyl HCH bend (C1)	
			1387	1398	sym methyl HCH bend (C5)	
1410m,br	1456s		1427	1434	in-phase cis =CH in-plane bend + asym methyl HCH bend (C1)	
1460s,br			1451	1457	asym methyl HCH bend (C1)	
			1456	1455	methylene scissors	
			1467	1467	asym methyl HCH bend (C1)	
			1471	1483	asym methyl HCH bend (C5)	
			1479	1493	asym methyl HCH bend (C5) + methylene scissors	
1662m	1658vs		1725	1731	C=C stretch	
			3010	2998	sym methylene stretch	
2889vs,br			3018	3019	sym methyl stretch (C1)	
			3028	3037	sym methyl stretch (C5)	
			3063	3058	asym methyl stretch (C1)	
			3075	3016	asym methylene stretch + asym methyl stretch (C5)	
			3099	3101	asym methyl stretch (C5)	
2947vs			3103	3112	asym methyl stretch (C5)	
2975vs			3115	3174	asym methyl stretch (C1) + out-of-phase =CH stretches	
			3122	3107	out-of-phase =CH stretch + asym methyl stretch (C1)	
3022vs			3146	3133	in-phase =CH stretch	

^a s, strong; m, medium; w, weak; sh, shoulder; br, broad; v, very; sym, symmetric; asym, antisymmetric; TAM, transverse acoustic mode.

overestimate the transition energy of the C=C stretch. A sharp band is seen at 1643 cm⁻¹ in the Raman spectrum (Figure 5), and the associated band is recorded in the infrared spectrum at 1648 cm⁻¹ (Figure 6). However, the DFT calculations predict a band at 1702 ± 2 cm⁻¹ for all four conformers. This overestimation of the C=C stretch is consistently observed with all the mono- and dienes investigated here.

cis-2-Pentene. *cis*-2-Pentene has been studied in the gas phase by microwave spectroscopy²⁷ and electron diffraction²⁸ and in the liquid and solid states by infrared and Raman spectroscopies²⁶ in the spectral region below 700 cm⁻¹. All studies concur that the

only conformer present is the skew form ($\angle \text{C}2\text{—C}3\text{—C}4\text{—C}5 = 120^\circ$). A potential energy scan of the rotation about the C3—C4 bond, (Figure 7) shows that the cis conformer ($\angle \text{C}2\text{—C}3\text{—C}4\text{—C}5 = 0^\circ$) is at much higher energy than the skew conformer (cis-skew = 16.3 kJ mol⁻¹ (B3LYP)) with a very low barrier of 1.47 kJ mol⁻¹ (ca. 0.5kT at 300 K); thus, it is both energetically unlikely and only metastable if formed. A vibrational analysis confirms that it is a stable structure (no imaginary modes).

A comparison of the observed and calculated structural parameters is given in Table S3, Supporting Information. The strain in

Table 4. Measured and Calculated Vibrational Energies with Assignments for *trans*-2-Pentene^a

experimental/cm ⁻¹			DFT/cm ⁻¹		assignment
infrared (gas phase, 323 K)	Raman (liquid, ~300 K)	INS (solid, 20 K)	skew conformer	cis conformer	
			95	137	C3–C4 torsion
			175	205	skeletal def. (pseudo-TAM)
			205	296	C5 methyl torsion
			214	232	C1 methyl torsion
			303	208	C2–C3–C4 bend
412m			409	583	C3–C4–C5 bend
488s			488	367	C1–C2–C3 bend
751w			758	714	out-of-phase trans =CH out-of-plane bend
799w			808	827	methylene rock
877w			881	859	in-phase C–C stretch (C3–C4, C4–C5) + methyl rock (C1)
957s	943w		950	951	methyl rock (C1) + out-of-phase C–C stretch (C1–C2, C4–C5)
969s			985	998	in-phase trans =CH out-of-plane bend
1024vw	1018vw		1026	1089	out-of-phase C–C stretch (C3–C4, C4–C5)
			1055	1057	methyl rock (C1)
1076w	1062m		1078	1028	methyl rock (C5) + in-phase C–C stretch (C1–C2, C4–C5)
			1098	1142	methyl rock (C5) + out-of-phase C–C stretch (C1–C2, C3–C4)
	1153vw		1172	1097	in-phase C–C stretches (C1–C2, C3–C4)
	1246w		1263	1277	methylene twist
1292w	1309s		1307	1315	in-phase trans =CH in-plane bend
	1335vw		1327	1335	out-of-phase trans =CH in-plane bend
1342w			1356	1361	methylene wag
1389w			1387	1391	sym methyl HCH bend (C5)
			1392	1399	sym methyl HCH bend (C1)
			1450	1452	asym methyl HCH bend (C1)
	1450s		1458	1460	methylene scissors
1467m			1467	1469	asym methyl HCH bend (C1)
			1470	1474	asym methyl HCH bend (C5)
			1479	1483	asym methyl HCH bend (C5) + methylene scissors
	1673vs		1737	1737	C=C stretch
2878vs			3008	3002	sym methylene stretch
2897vs			3013	3012	sym methyl stretch (C1)
2940vs			3027	3031	sym methyl stretch (C5)
			3058	3020	asym methylene stretch
			3062	3061	asym methyl stretch (C1)
2970vs			3096	3099	asym methyl stretch (C5)
			3099	3099	asym methyl stretch (C1)
			3103	3104	asym methyl stretch (C5)
3030vs			3113	3119	=C3–H stretch
			3126	3150	=C2–H stretch

^a s, strong; m, medium; w, weak; sh, shoulder; br, broad; v, very; sym, symmetric; asym, antisymmetric; TAM, transverse acoustic mode.

the cis conformer produced by the close proximity of the methyl groups strongly distorts the carbon atom skeleton, opening the CCC bond angles along the carbon atom backbone. All CCC bond angles increase significantly: $\angle \text{C}1\text{--C}2\text{=C}3$ 128.0° vs 131.5°, $\angle \text{C}2\text{=C}3\text{--C}4$ 128.2° vs 133.6°, and $\angle \text{C}3\text{--C}4\text{--C}5$ 112.4° vs 120.1° for the skew and cis conformers, respectively. The C–H, C=C, and C–C bond distances are essentially identical in the two species, and both H–C–H angles are approximately tetrahedral with no difference between the conformers.

Figure 8 shows the experimental spectra compared to those calculated for the skew and cis conformers, and the transition

energies and assignments are given in Table 3. The spectra in all three states are consistent with only the exclusive existence of the skew conformer. The microwave study concluded that the energy separation for the lowest vibrational mode is $68 \pm 12 \text{ cm}^{-1}$ for the $2 \leftarrow 0$ transition of the C3–C4 torsion, in fair agreement with the prediction of $92 (= 2 \times 46) \text{ cm}^{-1}$ from Table 3.

trans-2-Pentene. *trans*-2-Pentene has been studied in the gas phase by electron diffraction²⁹ and in the liquid and solid states by infrared spectroscopy²⁶ in the spectral region below 700 cm⁻¹. The vibrational spectra clearly show the presence of

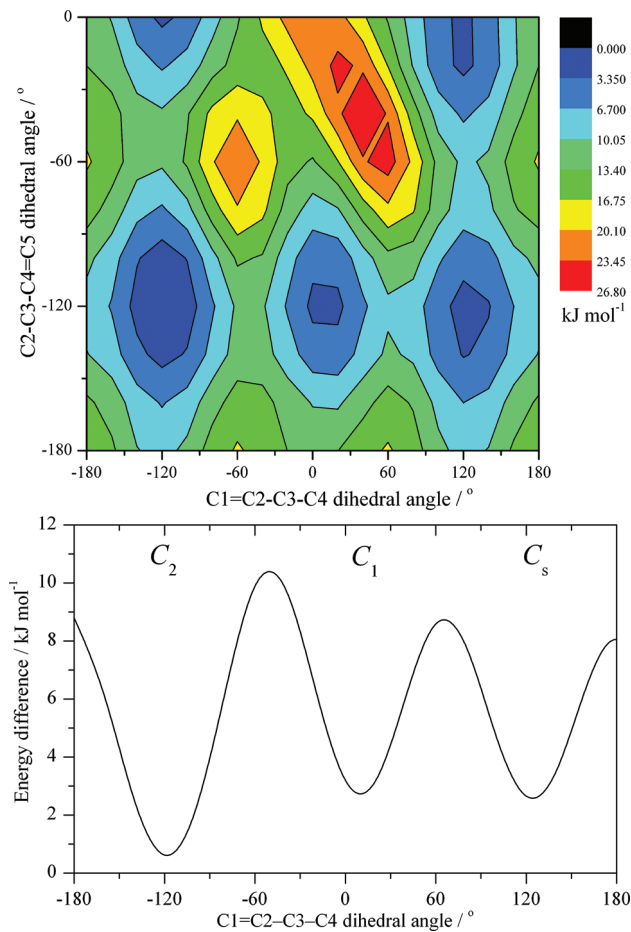


Figure 13. (Top) Potential energy surface for 1,4-pentadiene as a function of rotation about the C2–C3 and C3–C4 bonds. (Bottom) Cut at $\angle \text{C}2\text{--C}3\text{--C}4\text{--C}5 = -120^\circ$ through the potential energy surface. C_2 (**14**), C_1 (**15**), and C_s (**16**) conformers are found at -118.2° , 10.0° , and 124.0° , respectively. (The C_2 conformer is not at zero energy because the dihedral angle is almost but not exactly -120° . The cut is the closest that the data would allow to the minima; thus, the barriers shown are slight underestimates of the true heights).

two conformers. A potential energy scan of the rotation about the C3–C4 bond (Figure 7) shows that the cis ($\angle \text{C}2\text{--C}3\text{--C}4\text{--C}5 = 0^\circ$) conformer is at slightly higher energy than the skew ($\angle \text{C}2\text{--C}3\text{--C}4\text{--C}5 = 120^\circ$) conformer (cis-skew = 2.48 kJ mol^{-1} (B3LYP)) (ca. kT at 300 K); thus, the cis conformer is present in significant quantities at room temperature, as found experimentally.²⁶

The INS spectrum, Figure 9a, shows only the skew conformer. In this case, the compound has crystallized, as shown by the sharp lattice modes below 200 cm^{-1} , rather than formed a glass. In the Raman spectrum, Figure 9b, the cis conformer is present as evidenced by the bands observed at 370 , 575 , and 852 cm^{-1} . In contrast to earlier infrared work,²⁶ we find, Figure 9c, surprisingly little evidence for the presence of the cis conformer, largely because its infrared spectrum is very similar to that of the skew conformer. The band at 575 cm^{-1} , which was previously used as a characteristic marker for the cis conformer, is absent in our spectrum. The associated vibrational mode is calculated to have a very low infrared intensity, so its presence in the earlier study is difficult to account for. The transition energies and assignments are given in Table 4.

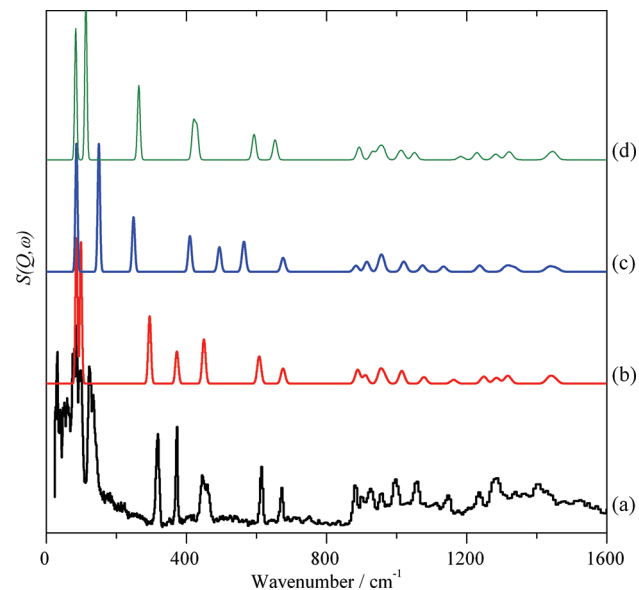


Figure 14. Comparison of (a) measured and calculated INS spectra of 1,4-pentadiene, (b) conformer 1 (**14**), (c) conformer 2 (**15**), and (d) conformer 3 (**16**).

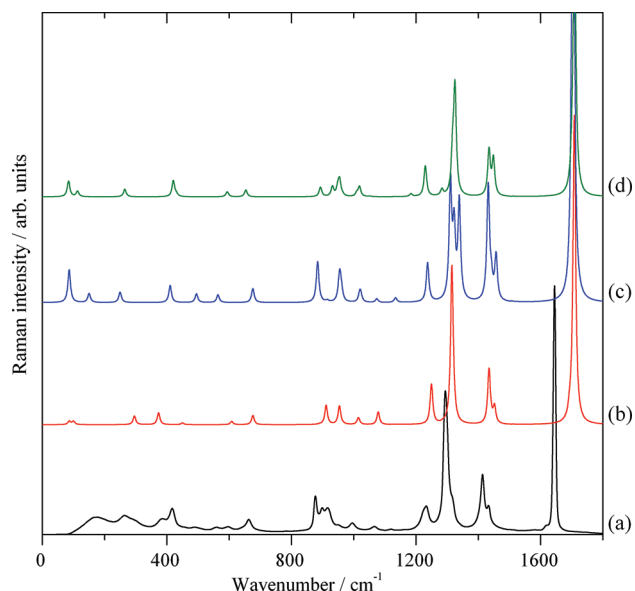


Figure 15. Comparison of (a) measured and calculated Raman spectra of 1,4-pentadiene, (b) conformer 1 (**14**), (c) conformer 2 (**15**), and (d) conformer 3 (**16**).

cis- and trans-1,3-Pentadiene. Both *cis*- and *trans*-1,3-pentadiene have been studied in the gas phase by microwave spectroscopy³⁰ and in the gas, liquid, and solid states by infrared and Raman spectroscopies.^{31,32} All studies conclude that for both compounds the only conformer present is the s-trans form ($\angle \text{C}1\text{--C}2\text{--C}3\text{--C}4 = 0^\circ$). A potential energy scan of the rotation about the C2–C3 bond, Figure 10, is in complete agreement with this conclusion. The s-cis conformer ($\angle \text{C}1\text{--C}2\text{--C}3\text{--C}4 = 180^\circ$) is a transition state, but as with *trans*-2-pentene, the skew conformer ($\angle \text{C}1\text{--C}2\text{--C}3\text{--C}4 = 180 \pm x^\circ$: $x = 34.1^\circ$ cis, 39.1° trans^o) for both isomers is stable (no imaginary modes) but is 16.4 and 15.1 kJ mol^{-1} (i.e., $>6kT$ at

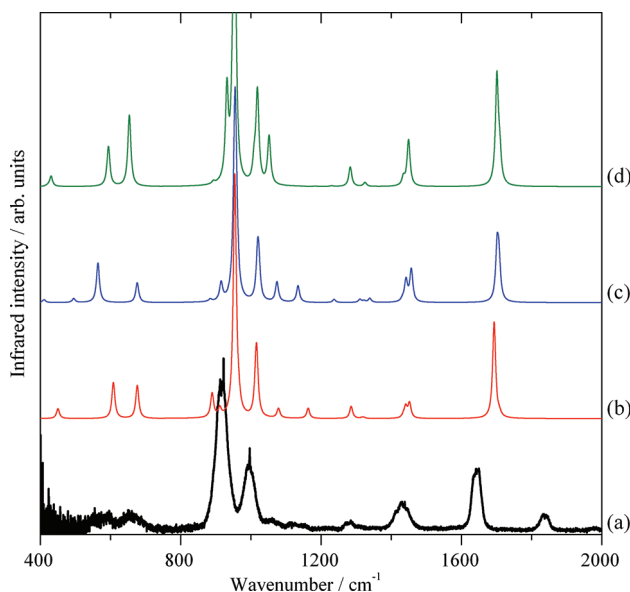


Figure 16. Comparison of (a) measured and calculated infrared spectra of 1,4-pentadiene, conformer 1 (**14**), (c) conformer 2 (**15**), and (d) conformer 3 (**16**).

300 K) higher in energy than the s-trans conformer for *cis*- and *trans*-1,3-pentadiene, respectively, and thus is not observed in the present work. Table S4, Supporting Information, compares the observed and calculated structures.

A comparison of the observed and calculated spectra is given in Figures 11 and 12 for *cis*- and *trans*-1,3-pentadiene, respectively. The experimental data for *cis*-1,3-pentadiene are of lower quality than usual because we were unable to obtain a pure sample of this compound. The spectra shown are generated by subtraction of the spectrum of pure *trans*-1,3-pentadiene from that of a technical mixture of *cis*- and *trans*-1,3-pentadiene (nominally 35% *cis*, 65% *trans*).

The spectra of *cis*- and *trans*-1,3-pentadiene have been comprehensively assigned previously,³² and our assignments, see Tables S5 and S6, Supporting Information, are largely in agreement with this work. Where disagreements occur (highlighted in red in Tables S5 and S6, Supporting Information), these are largely for modes that are very weak in the infrared or Raman spectra and are generally in the low-energy region of the spectrum. It is exactly in this region that INS spectroscopy excels and emphasizes the need for all three types of vibrational spectra in combination with DFT calculations for a complete assignment.

1,4-Pentadiene. 1,4-Pentadiene presents a similar conformational problem to that of 1-pentene in that there are two torsions that need to be considered (about the C2–C3 and C3–C4 bonds). The potential energy landscape has been investigated by molecular mechanics³³ and by a SCF MO LCAO scheme using a minimal basis of contracted Gaussian functions.³⁴ Our DFT calculations of the system are shown in Figure 13(top) and are in general agreement with the earlier less sophisticated calculations. Three minima are apparent at (−118.2, −118.2), (10.0, −119.5), and (124.0, −124.0); these are a C_2 , C_1 , and C_s conformer, respectively. (The minima at (−119.5, 10.0) and (119.5, −10.0) are identical by symmetry to the minimum at (10.0, −119.5).) DFT calculations identify the C_2 conformer as the lowest energy form with the C_1 (3.18 kJ mol^{−1}) and C_s (1.43 kJ mol^{−1}) conformers slightly higher in energy. MP2 calculations indicate

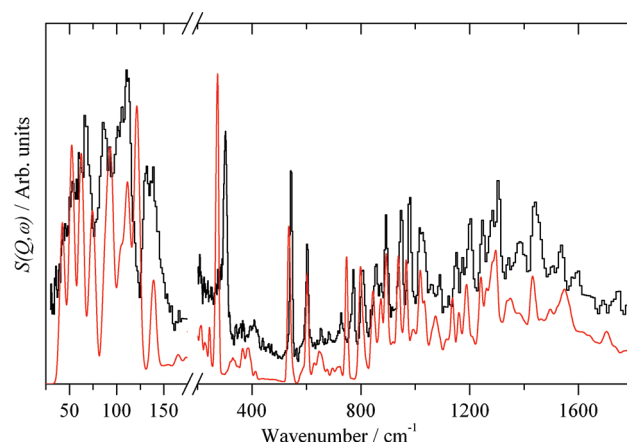


Figure 17. Comparison of measured (black line) and CASTEP-calculated (red line) INS spectrum of cyclopentane (**17**). Note that the right-hand side of the figure is $\times 3$ ordinate expanded relative to the left.

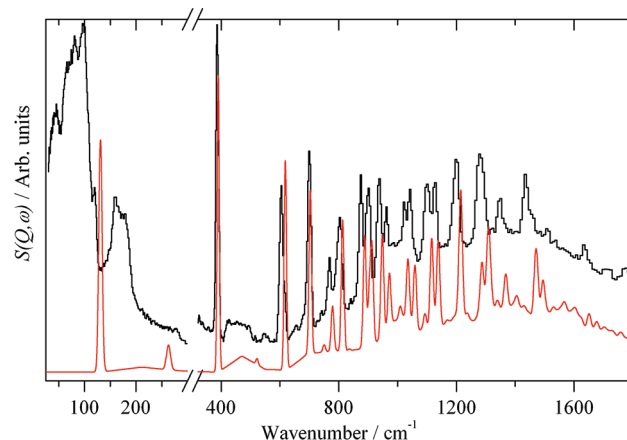


Figure 18. Comparison of measured (black line) and calculated (red line) INS spectrum of cyclopentene (**18**). Note that the right-hand side of the figure is $\times 2$ ordinate expanded relative to the left.

somewhat larger differences: C_1 (3.97 kJ mol^{−1}) and C_s (2.39 kJ mol^{−1}). A cut at $\angle C2-C3-C4=C5 = -120^\circ$ is shown in Figure 13(bottom) and indicates that the barriers to interconversion are significant: $\sim 3-4kT$ at 300 K. Thus, at room temperature in a fluid state all three conformers can reasonably be expected to be present.

Comparison of the calculated barriers to those of the C5 alkenes and dienes (Figures 7, 10, and 13(bottom)) strikingly shows the effect of conjugation. The barriers for interconversion of the conformers of the 1,3-pentadienes are 2–3 times larger than those for the conformers of the alkenes or 1,4-pentadiene.

Experimentally, 1,4-pentadiene has been investigated in the gas phase by electron diffraction^{33,35} and microwave spectroscopy³⁶ and in the gas,³⁷ liquid,^{34,37} and solid^{34,37} states by infrared and Raman spectroscopy. Microwave spectroscopy³⁶ was only able to determine rotational constants for one conformer. Consideration³⁷ of all three conformers suggested that the observed rotational constants best fitted the C_1 conformer, a result confirmed by the present work (Table S7, Supporting Information). Electron diffraction data were consistent with the presence of multiple conformers which could be modeled either as a semirigid molecule³³ or as a mixture of all three conformers.³⁵

Table 5. Measured and Calculated Vibrational Energies with Assignments for Conformers 1 (C_2), 2 (C_1), and 3 (C_s) of 1,4-Pentadiene^a

experimental/cm ⁻¹			DFT/cm ⁻¹		
infrared (gas phase, 323 K)	Raman (liquid, ~300 K)	INS (solid, 20 K)	conformer 1 (C_2)	conformer 2 (C_1)	conformer 3 (C_s)
596w	123vs	86	86	84	disrotatory C2—C3 torsion + C3—C4 torsion
	134s	100	150	113	conrotatory C2—C3 torsion + C3—C4 torsion
	263m, 295sh	318s	296	250	C2—C3—C4 bend
	383m415m	374s	373	411	in-phase C1=C2—C3 bend + C3—C4=C5 bend
	492w	445/461m	450	495	out-of-phase C1=C2—C3 bend + C3—C4=C5 bend
	557/596w	615	608	564	=C1H ₂ , =C2H ₃ out-of-plane bend in phase with =C4H ₆ , =C5H ₇ out-of-plane bend
	663m	673	676	654	=C1H ₂ , =C5H ₂ out-of-phase twist
	877m	881m	890	884	=C1H ₂ , =C5H ₂ in-phase rock
		900w	911	915	=C1H ₂ , =C5H ₂ out-of-phase rock
	915s	898m	926m	954	=C1H ₂ , =C5H ₂ out-of-phase wag
915s	917m	926m	955	956	=C1H ₂ , =C5H ₂ in-phase wag
		955m	966	961	out-of-phase C—C stretches (C2—C3, C3—C4)
	997w	999m	1014	1019	=C2H ₃ out-of-plane bend in phase with =C4H ₆ out-of-plane bend
	999s	997w	999m	1017	=C2H ₃ out-of-plane bend out-of-phase with =C4H ₆ out-of-plane bend
		1078w	1057m	1079	in-phase C—C stretches (C3—C4, C3—C4)
	1120vw	1147m	1163	1134	methylene rock
	1233m	1237m	1250	1237	methylene twist
	1277w	1282s,br	1286	1311	methylene wag
		1293vs	1315	1322	=C2H ₃ in-plane bend in phase with =C4H ₆ in-plane bend
	1314w		1320	1338	=C2H ₃ in-plane bend out of phase with =C4H ₆ in-plane bend
1434m	1414s	1406m,br	1434	1432	=C1H ₂ , =C5H ₂ out-of-phase scissors + methylene scissors
			1441	1442	=C1H ₂ , =C5H ₂ in-phase scissors
	1433w		1452	1457	methylene scissors + =C1H ₂ , =C5H ₂ out-of-phase scissors
			1693	1702	out-of-phase C=C stretch
1645s	1644vs		1708	1706	in-phase C=C stretch
			3013	1995	sym methylene stretch
			3057	3032	asym methylene stretch
			3133	3133	out-of-phase sym vinyl CH ₂ stretch
			3133	3136	in-phase sym vinyl CH ₂ stretches
			3144	3142	out-of-phase =C2H ₃ , =C4H ₆ stretch
			3145	3148	in-phase =C2H ₃ , =C4H ₆ stretch
			3226	3226	in-phase asym vinyl CH ₂ stretches
			3226	3233	out-of-phase asym vinyl CH ₂ stretch

^a s, strong; m, medium; w, weak; sh, shoulder; br, broad; v, very; sym, symmetric; asym, antisymmetric.

Our calculated structural parameters are in good agreement with those observed experimentally (Table S7, Supporting Information).

The vibrational spectra confirm the modeling, and three conformers have been identified in the gas and liquid states,^{34,37} although the assignments differ. The spectrum of the annealed solid is consistent with the presence of only one conformer, identified as the C_2 species,³⁷ in agreement with our DFT calculations identifying this as the lowest energy conformer. A comparison

of the observed and calculated INS, Raman, and infrared spectra of the conformers is shown in Figures 14–16, and the observed and calculated transition energies and assignments are presented in Table 5.

Our spectra are in general agreement with those in the literature. The measured INS spectrum, Figure 14, shows that apart from the two lowest lying torsions (which will be strongly influenced by neighboring molecules) there is good agreement with the calculated spectrum of the C_2 conformer. The absence of

a band near 250 cm^{-1} indicates that the other two conformers are absent. The sharp lattice modes below 110 cm^{-1} are consistent with a crystalline solid, suggesting the existence of only one conformer. In the Raman spectrum (Figure 15) the presence of the three conformers is indicated by the multiple bands observed at approximately 900 , 600 , and 400 cm^{-1} . The infrared spectra (Figure 16) of all three conformers are similar, making it difficult to positively identify them.

Cyclopentane. Cyclopentane has attracted a great deal of attention both theoretically^{38–41} and experimentally.^{42–52} The planar D_{5h} structure of cyclopentane is not an energy minimum but a saddle point on the potential energy surface, and to reduce its energy the molecule is puckered in all three physical states. The puckered state has two isoenergetic forms, a C_s and a C_2 structure, each with several states that are only distinguishable if the atoms are labeled. The nuclear motions resulting from interconversion between these forms can be compared to almost free rotation of a particle on a ring, referred to as pseudorotation, and can be regarded as a special form of anharmonicity. It was introduced by Kilpatrick, Pitzer, and Spitzer³⁸ to explain the diffuseness of the symmetric C–C stretching mode in the vibrational spectrum of cyclopentane and also why the experimental entropy and specific heat of cyclopentane was smaller than predicted by the harmonic oscillator rigid rotator model. The pseudorotation derives from one of the doubly degenerate out-of-plane ring vibrations of the planar D_{5h} structure; the other mode is best described as a radial vibration which is a nearly harmonic vibration in which the amount of puckering oscillates about an equilibrium value.

The unusual nature of the pseudorotation ‘vibration’ results in one imaginary mode for the energy-minimized structure, since it is outside of the harmonic approximation. The calculated structure is in reasonable agreement with the limited structural data available for the gas phase^{42,43} and also for the low-temperature solid phase III⁴⁴ (Table S8, Supporting Information). Our infrared and Raman spectra are shown in Figure S2, Supporting Information, and the assignments are in complete agreement with the literature^{45–50} and are given in Table S9, Supporting Information.

In the solid state, cyclopentane undergoes pseudorotation in the plastic phases I and II. However, it is frozen out in phase III, which occurs below 118 K , so that the pseudorotation and the radial vibration revert to conventional out-of-plane bending modes. These are predicted⁴⁹ to occur at 135 and 242 cm^{-1} , respectively; thus, they should be apparent in the INS spectrum. A low-resolution INS spectrum of the restricted energy transfer range has been reported.⁵² Peaks at 136 and 303 cm^{-1} are consistent with the prediction but may also be assigned to lattice modes. To clarify this point we carried out periodic-DFT calculations of the complete unit cell using the CASTEP code, with the lattice parameters fixed at the experimental values.⁴⁴ A comparison of our higher resolution INS spectrum with that predicted from CASTEP is shown in Figure 17. It is evident that there is reasonable agreement between the observed and the CASTEP spectra. From visualization of the modes we can confirm that the bands at 131 , 139 , and 300 cm^{-1} originate in the ring puckering modes.

Cyclopentene. Cyclopentene has also been extensively studied.^{53–63} The molecule is puckered, C_s symmetry, and most investigations have been aimed at determining the nature of the ring puckering vibration and the barrier to inversion of the ring. The calculated structure is in reasonable agreement with the limited structural data available for the gas phase^{53–56} (Table S8, Supporting Information). Similarly, the assignments of the infrared and Raman spectra (Table S10 and Figure S3,

Supporting Information) are in general agreement with the latest literature work,⁶³ except for three minor disagreements (900 , 1140 , 1208 cm^{-1}), which we attribute to application of a basis set that did not include diffuse functions.

The INS spectrum, Figure 18, has not been reported previously; unfortunately, neither is the crystal structure known. An infrared and a Raman investigation⁶¹ suggested that the low-temperature phase (below 87 K) was orthorhombic and noncentrosymmetric with four molecules in the unit cell. The puckering mode centered at 169 cm^{-1} shows structure at 159 and 179 cm^{-1} consistent with this suggestion.

CONCLUSIONS

One of the surprises of this work was how well behaved all the species were in the sense that the observed transition energies fall within the ranges expected from group frequency tables.^{64,65} This is despite the fact that the mode visualizations show the descriptions to be large oversimplifications of the true dynamics.

It has been noted^{7,66,67} on many occasions that comparison of calculated and experimental vibrational spectra is a more stringent test of theory than just a comparison of calculated and observed structures. It is well documented^{68,69} that the vibrational assignments provided by DFT are generally in excellent agreement with experiment; however, there are clearly still areas for improvement as shown by the $\text{C}=\text{C}$ stretching mode consistently being calculated at too high an energy. Calculation of the relative energies of the conformers is also a good test as it depends on an accurate calculation of both the total energy and the vibrational energies (since the ZPE influences the result). It is clearly essential to have reliable data to test theory against.

The work also highlights the potential of the use of gas-phase infrared spectroscopy for catalysis studies.^{4,5} The ability to obtain quantifiable real-time data as well as provide not only molecular discrimination but isomer and conformer discrimination is a very powerful combination that deserves exploitation. It is also evident that the greatest discrimination occurs in the low-wavenumber region 200 – 800 cm^{-1} . This is not the simplest spectral region to access experimentally; however, the relative scarcity of modes in this region renders its use very attractive.

ASSOCIATED CONTENT

S Supporting Information. Chemical structures, conformations, and point groups of the C_5 species, comparison of measured and calculated Raman and infrared spectra of cyclopentane and cyclopentene; comparison of experimental and calculated structural parameters for the molecules considered; experimental and calculated transition energies with assignments for 10–13, 17, and 18. This material is available free of charge via the Internet at <http://pubs.acs.org>.

AUTHOR INFORMATION

Corresponding Author

*E-mail: stewart.parker@stfc.ac.uk.

Present Addresses

[§] Reactivity Group, Abteilung Anorganische Chemie, Fritz-Haber-Institut der Max-Planck-Gesellschaft, Faradayweg 4–6, 14195 Berlin, Germany.

[¶] Present address: Palacky University in Olomouc, Faculty of Science, Department of Optics, 17 Listopadu 1192/12, Olomouc, 77146, Czech Republic.

■ ACKNOWLEDGMENT

The authors thank the STFC Rutherford Appleton Laboratory for access to neutron beam facilities. Computing resources (time on the SCARF computer used to perform the CASTEP calculations and some of the Gaussian 03 calculations) were provided by STFC's e-Science facility.

■ REFERENCES

- (1) Weissermel, K.; Arpe, H.-J. *Industrial Organic Chemistry*, 3rd ed.; VCH: Weinheim, 1997.
- (2) Webb, G. In *Catalysis, Specialist Periodical Reports*; Kemball, C., Dowden, D. A., Eds.; The Chemical Society: London, 1978; Vol. 2, p 145.
- (3) Matyshak, V. A.; Krylov, O. V. *Catal. Today* **1995**, *25*, 1.
- (4) Opara, E.; Lundie, D. T.; Lear, T.; Sutherland, I. W.; Parker, S. F.; Lennon, D. *Phys. Chem. Chem. Phys.* **2004**, *6*, 5588.
- (5) McFarlane, A.; McMillan, L.; Silverwood, I. P.; Hamilton, N. G.; Siegel, D.; Parker, S. F.; Lundie, D. T.; Lennon, D. *Catal. Today* **2010**, *155*, 206.
- (6) Hecht, L.; Barron, L. D.; Blanch, E. W.; Bell, A. F.; Day, L. A. *J. Raman Spectrosc.* **1999**, *30*, 815.
- (7) Mitchell, P. C. H.; Parker, S. F.; Ramirez-Cuesta, A. J.; Tomkinson, J. *Vibrational Spectroscopy With Neutrons, With Applications in Chemistry, Biology, Materials Science and Catalysis*; World Scientific: Singapore, 2005.
- (8) Colognesi, D.; Celli, M.; Cillico, F.; Newport, R. J.; Parker, S. F.; Rossi-Albertini, V.; Sacchetti, F.; Tomkinson, J.; Zoppi, M. *Appl. Phys. A: Mater. Sci. Process.* **2002**, *74* (Suppl.), S64.
- (9) <http://www.isis.stfc.ac.uk/>.
- (10) Frisch, M. J.; Trucks, G. W.; Schlegel, H. B.; Scuseria, G. E.; Robb, M. A.; Cheeseman, J. R.; Montgomery, J. A., Jr.; Vreven, T.; Kudin, K. N.; Burant, J. C.; Millam, J. M.; Iyengar, S. S.; Tomasi, J.; Barone, V.; Mennucci, B.; Cossi, M.; Scalmani, G.; Rega, N.; Petersson, G. A.; Nakatsuji, H.; Hada, M.; Ehara, M.; Toyota, K.; Fukuda, R.; Hasegawa, J.; Ishida, M.; Nakajima, T.; Honda, Y.; Kitao, O.; Nakai, H.; Klene, M.; Li, X.; Knox, J. E.; Hratchian, H. P.; Cross, J. B.; Adamo, C.; Jaramillo, J.; Gomperts, R.; Stratmann, R. E.; Yazyev, O.; Austin, A. J.; Cammi, R.; Pomelli, C.; Ochterski, J. W.; Ayala, P. Y.; Morokuma, K.; Voth, G. A.; Salvador, P.; Dannenberg, J. J.; Zakrzewski, V. G.; Dapprich, S.; Daniels, A. D.; Strain, M. C.; Farkas, O.; Malick, D. K.; Rabuck, A. D.; Raghavachari, K.; Foresman, J. B.; Ortiz, J. V.; Cui, Q.; Baboul, A. G.; Clifford, S.; Cioslowski, J.; Stefanov, B. B.; Liu, G.; Liashenko, A.; Piskorz, P.; Komaromi, I.; Martin, R. L.; Fox, D. J.; Keith, T.; Al-Laham, M. A.; Peng, C. Y.; Nanayakkara, A.; Challacombe, M.; Gill, P. M. W.; Johnson, B.; Chen, W.; Wong, M. W.; Gonzalez, C.; Pople, J. A. *Gaussian 03, Revision B.05*; Gaussian, Inc.: Pittsburgh, PA, 2003.
- (11) Ramirez-Cuesta, A. J. *Comput. Phys. Commun.* **2004**, *157*, 226.
- (12) Snyder, R. G.; Schachtschneider, J. H. *Spectrochim. Acta* **1963**, *19*, 85.
- (13) Shimanouchi, T.; Matsuura, H.; Ogawa, Y.; Harada, I. *J. Phys. Chem. Ref. Data* **1978**, *7*, 1323.
- (14) Braden, D. A.; Parker, S. F.; Tomkinson, J.; Hudson, B. S. *J. Chem. Phys.* **1999**, *111*, 429.
- (15) Tomkinson, J.; Parker, S. F.; Braden, D. A.; Hudson, B. S. *Phys. Chem. Chem. Phys.* **2002**, *4*, 716.
- (16) Mirkin, N. G.; Krimm, S. *J. Phys. Chem.* **1993**, *97*, 13887.
- (17) Bower, D. I.; Maddams, W. F. *The Vibrational Spectroscopy of Polymers*; Cambridge University Press: Cambridge, 1989.
- (18) Barnes, J.; Franconi, B. *J. Phys. Chem. Ref. Data* **1978**, *7*, 1309.
- (19) Mathisen, H.; Norman, N.; Pedersen, B. F. *Acta Chem. Scand.* **1967**, *21*, 127.
- (20) Goodman, M. A.; Sweany, R. L.; Flurry, R. L., Jr. *J. Phys. Chem.* **1983**, *87*, 1753.
- (21) Balabin, R. M. *J. Phys. Chem. A* **2009**, *113*, 1012.
- (22) Parker, S. F. *Spectrochim. Acta A* **2006**, *63*, 544.
- (23) Fraser, G. T.; Xu, L.-H.; Suenram, R. D.; Lugez, C. L. *J. Chem. Phys.* **2000**, *112*, 6209.
- (24) Linares, M.; Pellegatti, A.; Roussel, C. *J. Mol. Struct. (THEOCHEM)* **2004**, *680*, 169.
- (25) Harragh, L. A.; Mayo, D. W. *J. Chem. Phys.* **1960**, *33*, 298.
- (26) Shimanouchi, T.; Abe, Y.; Alaki, Y. *Polym. J.* **1971**, *2*, 199.
- (27) Van Eijck, B. P. *J. Mol. Spectrosc.* **1981**, *85*, 189.
- (28) Ter Brake, J. H. M. *J. Mol. Struct.* **1984**, *118*, 63.
- (29) Ter Brake, J. H. M.; Mijlhoff, F. C. *J. Mol. Struct.* **1981**, *77*, 253.
- (30) Hsu, S. L.; Flygare, W. H. *J. Chem. Phys.* **1970**, *52*, 1053.
- (31) Rasmussen, R. S.; Brattain, R. R. *J. Chem. Phys.* **1947**, *15*, 131.
- (32) Compton, D. A. C.; George, W. O.; Maddams, W. F. *J. Chem. Soc., Perkin Trans. II* **1977**, 1733.
- (33) Van Eijck, B. P. *J. Mol. Struct.* **1984**, *118*, 73.
- (34) Gallinella, E.; Cadioli, B. *J. Chem. Soc., Faraday Trans. 2* **1975**, *71*, 781.
- (35) McClelland, B. W.; Hedberg, K. *J. Am. Chem. Soc.* **1987**, *109*, 7304.
- (36) Unpublished results from Hirota, E. cited in Cadioli, B.; Gallinella, E. *J. Mol. Struct.* **1976**, *31*, 199.
- (37) Inagaki, F.; Sakakibara, M.; Harada, I.; Shimanouchi, T. *Bull. Chem. Soc. Jpn.* **1975**, *48*, 3557.
- (38) Kilpatrick, J. E.; Pitzer, K. S.; Spitzer, R. *J. Am. Chem. Soc.* **1947**, *69*, 2483.
- (39) Tomimoto, M.; Go, N. *J. Phys. Chem.* **1995**, *99*, 563.
- (40) Han, S. J.; Kang, Y. K. *J. Mol. Struct. (THEOCHEM)* **1996**, *362*, 243.
- (41) Sax, A. F. *Chem. Phys.* **2008**, *349*, 9.
- (42) Almenningen, A.; Bastiansen, O.; Skancke, P. N. *Acta Chem. Scand.* **1961**, *15*, 711.
- (43) Adams, W. J.; Geise, H. J.; Bartells, L. S. *J. Am. Chem. Soc.* **1970**, *92*, 5013.
- (44) Torrisi, A.; Leech, C. K.; Shankland, K.; David, W. I. F.; Ibbsen, R. M.; Benet-Buchholz, J.; Boese, R.; Leslie, M.; Catlow, C. R. A.; Price, S. L. *J. Phys. Chem. B* **2008**, *112*, 3746.
- (45) Miller, F. A.; Inskeep, R. G. *J. Chem. Phys.* **1950**, *18*, 1519.
- (46) Durig, J. R.; Wertz, D. W. *J. Chem. Phys.* **1968**, *49*, 2118.
- (47) Schettino, V.; Marzocchi, M. P.; Califano, S. *J. Chem. Phys.* **1969**, *51*, 5264.
- (48) Carreira, L. A.; Jiang, G. J.; Person, W. B.; Willis, J. N. *J. Chem. Phys.* **1972**, *56*, 1440.
- (49) Schettino, V.; Marzocchi, M. P. *J. Chem. Phys.* **1972**, *57*, 4225.
- (50) Durig, J. R.; Hudgens, B. A.; Zhizhin, G. N.; Rogovoi, V. N.; Casper, J. M. *Mol. Cryst. Mol. Liq.* **1975**, *31*, 185.
- (51) Bauman, L. E.; Laane, J. *J. Phys. Chem.* **1988**, *92*, 1040.
- (52) Besnard, M.; Fouassier, M.; Lasseguès, J. C.; Dianoux, A. J.; Petry, W. *Mol. Phys.* **1991**, *73*, 1059.
- (53) Rathjens, G. W. *J. Chem. Phys.* **1962**, *36*, 2401.
- (54) Butcher, S. S.; Costain, C. C. *J. Mol. Spectrosc.* **1965**, *15*, 40.
- (55) Włodarczak, G.; Demaison, J. *J. Mol. Spectrosc.* **1992**, *155*, 143.
- (56) Davis, M. I.; Muecke, T. W. *J. Phys. Chem.* **1970**, *74*, 1104.
- (57) Laane, J.; Lord, R. C. *J. Chem. Phys.* **1967**, *47*, 4941.
- (58) Ueda, T.; Shimanouchi, T. *J. Chem. Phys.* **1967**, *47*, 5018.
- (59) Chao, T. H.; Laane, J. *J. Chem. Phys. Lett.* **1972**, *14*, 595.
- (60) Durig, J. R.; Carreira, L. A. *J. Chem. Phys.* **1972**, *56*, 4966.
- (61) Haines, J.; Gilson, D. F. R. *J. Phys. Chem.* **1989**, *93*, 20.
- (62) Cavagnat, D.; Cavagnat, R. M.; Cornut, J. C.; Banisaeid-Vahedie, S. *J. Phys.: Condens. Matter* **1992**, *4*, 4205.
- (63) Al-Saadi, A. A.; Laane, J. *J. Mol. Struct.* **2007**, *830*, 46.
- (64) Bellamy, L. J. *The Infrared Spectra of Complex Molecules*, 3rd ed.; Chapman and Hall: London, 1975.
- (65) Lin-Vien, D.; Colthup, N. B.; Fateley, W. G.; Grasselli, J. G. *The Handbook of Infrared and Raman Characteristic Frequencies of Organic Molecules*; Academic Press: San Diego, 1991.
- (66) Matsuura, H.; Yoshida, H. In *Handbook of Vibrational Spectroscopy*; Chalmers, J. M., Griffiths, P. R., Eds.; John Wiley & Sons: Chichester, 2002.
- (67) Kearley, G. J.; Johnson, M. R. *Vib. Spectrosc.* **2010**, *53*, 54.
- (68) Carbonniere, P.; Barone, V. *Chem. Phys. Lett.* **2004**, *399*, 226.
- (69) Meier, R. J. *Vib. Spectrosc.* **2007**, *43*, 26.